

Crossover behavior in the event size distribution of the Olami-Feder-Christensen model

G. Miller and C. J. Boulter

School of Mathematical and Computer Sciences, Department of Mathematics, Scott Russell Building, Heriot-Watt University, Edinburgh EH14 4AS, United Kingdom

(Received 21 November 2002; revised manuscript received 11 February 2003; published 21 April 2003)

The avalanche size distribution and supercritical toppling value distribution in the Olami-Feder-Christensen model are examined, demonstrating that there exists a crossover value $\alpha_c \approx 0.14$ for the conservation parameter in the model. We have further confirmed the location of this crossover by identifying upper and lower bounds for α_c . For levels of conservation below α_c the asymptotic behavior, in the limit of both infinite-system-size and infinite-precision arithmetic, consists only of avalanches of size 1 with all sites toppling exactly at the threshold value. For larger levels of conservation the probability of finding avalanches of size 2 or bigger remains nonzero in the asymptotic limit.

DOI: 10.1103/PhysRevE.67.046114

PACS number(s): 05.65.+b, 45.70.Ht, 05.45.Ra

I. INTRODUCTION

In recent years self-organized criticality (SOC) [1,2] has been introduced to provide an explanation for the ubiquitous presence of scale invariance in a range of naturally occurring systems. For example, in earthquakes and landslides the size distribution of events follows a power-law behavior over observable scales. In models where the dynamical variables are locally conserved there is analytic evidence of scale invariant behavior [3], however, the situation is less clear in models with nonconservation. The most studied nonconservative SOC model was introduced by Olami, Feder, and Christensen (OFC) [4] and is motivated by the Burridge-Knopoff spring-block description of earthquake dynamics [5].

In the OFC model [4], each node (i,j) on a square $L \times L$ lattice is associated with a continuous state variable or dimensionless energy u_{ij} . The system is slowly “driven” in such a way that the energies at all the sites increase uniformly until one of the sites reaches the threshold value, which can be chosen as $u_{th}=1$ without loss of generality. When this happens an avalanche occurs on a time scale much quicker than the driving speed. The supercritical site relaxes according to $u_{ij} \rightarrow 0$ with its energy distributed to the four neighbors u_{nn} using the rule $u_{nn} \rightarrow u_{nn} + \alpha u_{ij}$. The parameter α determines the level of conservation in the toppling process with $\alpha=0.25$ and $\alpha<0.25$ corresponding to conservative and dissipative systems, respectively. If any of the neighboring sites become supercritical (i.e., $u_{nn} \geq 1$) as a result of this procedure they also topple according to the same rules. The “avalanche” continues until all node values are below the threshold, at that stage the driving process proceeds until the next event is triggered.

Despite its apparent simplicity the OFC model displays a range of complex behavior. For the case where periodic boundary conditions are applied to the lattice it has been shown numerically that the system approaches a periodic state with all avalanches consisting of a single toppling site [6], at least for sufficiently small values of α [7]. This result is associated with a synchronization of sites in the system during the organizational process. Middleton and Tang [8] have given analytic support for this argument by examining

systems containing only two sites. More recently, Drossel [9] has provided evidence that in the limit of infinite-precision calculations the model with periodic boundary conditions indeed organizes to a periodic state with all avalanches being of size 1. The failure to observe this in some previous simulations can be directly attributed to a small level of desynchronization introduced by the use of limited precision arithmetic [9]. Thus, in the case of periodic boundary conditions the system is not critical, i.e., it does not display a scale-invariant avalanche size distribution.

The behavior is more complicated when open boundary conditions are used, with many questions remaining unresolved. The interior of the system tends to synchronize just as described above, however, the inhomogeneity introduced by the boundary sites (that have a different number of neighbors than the interior sites) prevents the creation of a completely periodic state. The resulting “marginal synchronization” may allow a critical state to develop for large enough values of α [2,7]. The model is critical in the conservative case, but is clearly not critical when $\alpha=0$ since all avalanches are of size 1, thus there must exist a critical value α_c such that the model is only critical when $\alpha \geq \alpha_c$. Early studies predicted $\alpha_c \approx 0.05$ [4], while simulations of larger lattices led Grassberger to the estimate $\alpha_c \geq 0.18$ [7]. More recent studies focusing on properties of the avalanche branching rates predict $\alpha_c = 0.25$ suggesting that the model is only critical in the conservative limit [10,11], although these findings remain controversial [12]. The prediction of Grassberger is based on the observations that for $\alpha < 0.18$ the avalanche distributions change qualitatively, resulting in an excess of small avalanches and a loss of scale invariance. A similar conclusion is drawn analytically by Bottani and Delamotte [13] when some simplifying assumptions concerning the avalanche dynamics and size distribution are employed. Furthermore, Drossel has conjectured that for small α the avalanche size distribution is again dominated by avalanches of size 1 [9]. In particular, in the asymptotic limit of both an infinite-size system ($L \rightarrow \infty$) and infinite precision, the distribution of avalanches of size greater than 1 is predicted to converge to zero, with all sites toppling exactly at the threshold value $u_{th} = 1$. Drossel concentrates on small values of the

conservation parameter $\alpha \leq 0.10$ and associates the results with the strong level of synchronization in the systems studied. This behavior cannot persist for all values of α if the model is critical in the conservative limit as assumed. Thus, in this paper we aim to check the findings of Drossel and identify the *crossover value* α_X below which the event size distributions are dominated by avalanches of size 1. That is, α_X is defined by demanding that the probability of finding an avalanche of size greater than 1 in the limit of both infinite-system size and infinite precision is zero for $\alpha < \alpha_X$ and non-zero for $\alpha \geq \alpha_X$. The crossover value also provides, by definition, a strict lower bound for α_c .

In Sec. II, we examine energy distributions and average toppling values within an avalanche. We find clear evidence for the existence of a crossover value at intermediate values of the conservation parameter and predict $\alpha_X \approx 0.14$. In Sec. III, we introduce two methods for strictly bounding the crossover value, which also allows us to test the effect of altering the floating-point precision used in the simulations. Our main results and conclusions are summarized in Sec. IV.

II. DISTRIBUTION FUNCTIONS

We start our investigation by examining the probability distribution P_d of energy differences between two neighboring sites. This is motivated by observations that within an avalanche the energy values of neighboring sites are often raised arbitrarily close to the threshold [9]. Thus, due to rounding effects caused by finite floating-point precision a sequence of avalanches of size 1 are mistaken for a larger single avalanche. Under this scenario the energy differences between nearest neighbors must typically be at multiples of α . This is plausible in the case $\alpha = 0.20$, as shown in Fig. 1 (lower curve) where it is clear there are peaks at multiples of 0.20 (as previously noted by Grassberger [7]). We further observe that as L increases the peaks become more pronounced, while the troughs reduce towards zero. However, moving towards the conservative regime we observe a different behavior. In Fig. 1 (upper curve), we show the results for $\alpha = 0.25$ where it is apparent that although there are clear peaks they are *not* at multiples of α , but rather at multiples of ≈ 0.31 . This suggests that although the seed sites all topple with energy value 1, further toppling sites will typically take supercritical values strictly greater than 1.

These results indicate that the crossover value $\alpha_X < 0.25$, but the possibility remains that $\alpha = 0.25$ is a special case with all nonconservative systems displaying similar behavior to $\alpha = 0.20$. To check, we have investigated values of α strictly between 0.20 and 0.25, and find that although there are peaks at the multiples of α there are also peaks at secondary values. As α is increased these extra peaks are found to become increasingly important. For example, our results for $\alpha = 0.24$ are shown in Fig. 1 (middle curve) where it is noted that the local maximums are ≈ 0.28 apart, with the front of these peaks being precisely at multiples of α . In this case, we believe that the broad humps seen are really two peaks with similar heights, sufficiently close to one another that they are observed as just one. For $\alpha < 0.24$ the individual peaks are more easily distinguished.

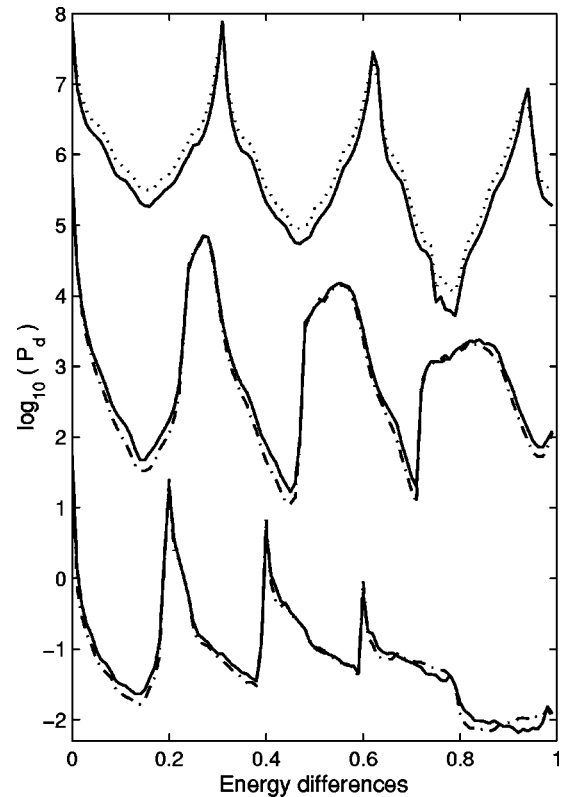


FIG. 1. Probability distributions P_d of energy differences between neighboring sites plotted on a logarithmic scale. From top to bottom the curves correspond to $\alpha = 0.25, 0.24$, and 0.20 . Results for systems of size $L = 700$ (solid) and $L = 1000$ (dash dot) are given, except for the case $\alpha = 0.25$ for which $L = 256$ (dotted) and $L = 700$ systems are shown. For clarity the $\alpha = 0.24$ and $\alpha = 0.25$ curves have been shifted upwards.

From the discussion above, we have shown that the distributions of energy differences between neighboring sites do not consist of peaks only at multiples of α , instead additional peaks are also seen for $\alpha > 0.20$. This appears in conflict with the concept of all sites toppling at the threshold value in the infinite-size limit. To further investigate, we analyze the probability distribution of supercritical toppling energy values u_{sc} directly. We find that for larger values of α , the majority of sites do not topple close to the threshold $u_{th} = 1$. In Fig. 2, we show the probability distributions P_{sc} of supercritical energy values for several choices of α .

When $\alpha = 0.25$ (upper curve), we observe a maximum at $u_{sc} \approx 1.25$. This maximum is consistent with our findings above for the distribution of energy differences between neighbors. Those distributions are “stationary,” i.e., one finds the same distribution for a given α at any period during the driving phase (in contrast the distribution of site energies u_{ij} is not generally stationary in the driving phase). Thus, for $\alpha = 0.25$ sites must typically receive multiples of ≈ 0.31 in order to retain the stationary distribution of peaks seen in Fig. 1. Therefore, a typical supercritical site will take a value of $u_{sc} \approx 1.25 \approx 4 \times 0.31$ or some larger multiple. In fact, as the system size is increased all peaks other than the one at 1.25 are found to diminish and in the limit $L \rightarrow \infty$ the probability distribution is predicted to consist of a δ function

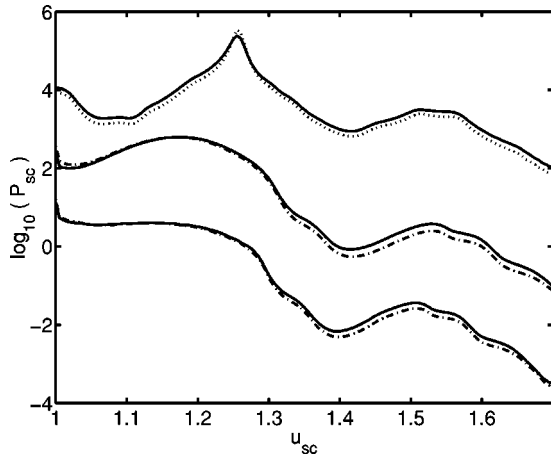


FIG. 2. Probability distributions P_{sc} of supercritical toppling energy plotted on a logarithmic scale. From top to bottom the curves correspond to $\alpha=0.25, 0.24$, and 0.23 . Results for systems of size $L=500$ (solid) and $L=1000$ (dash dot) are given, except for the case $\alpha=0.25$ for which the two largest systems simulated [$L=500$ and $L=700$ (dotted)] are shown. For clarity the $\alpha=0.24$ and $\alpha=0.25$ curves have been shifted upwards.

centered at $u_{sc} \approx 1.25$. The peak at $u_{sc}=1$ seen in Fig. 2 for finite-sized systems is related to the avalanche seed sites which topple precisely at the threshold value by definition. In the $L \rightarrow \infty$ limit the average avalanche size is predicted to diverge since the system is assumed critical, and hence the proportion of seed sites tends to zero in this limit.

For the case $\alpha=0.24$ there are two peaks, at $u_{sc}=1$ and 1.175 , both of approximately the same height as shown in Fig. 2 (middle curve). As $L \rightarrow \infty$ the distribution in the range $1 \leq u_{sc} \leq 1.35$ converges to a nonzero limit, with the distribution tending to zero for larger u_{sc} (the convergence is more convincingly seen when the distributions are plotted on a linear scale, we have used a logarithmic scale in Fig. 2 to reveal the distribution structure at larger values of u_{sc} which is not visible on a linear scale). As α is decreased the peak at 1 becomes more prominent, as demonstrated by the case $\alpha=0.23$ shown in Fig. 2 (lower curve). Once again there is a finite region ($1 \leq u_{sc} \leq 1.30$) in which the distribution remains nonzero in the limit $L \rightarrow \infty$. We believe from this that a crossover gradually occurs as α is decreased with the largest nonzero contribution of the $L \rightarrow \infty$ distribution tending towards one, and the relative height of the peak at 1 increases as α decreases. Even for the case $\alpha=0.20$ the distribution of supercritical values extends over a finite nonzero range as $L \rightarrow \infty$, indicating that a measurable proportion of supercritical sites do not topple at the threshold value in this limit. Thus, from our study of the distribution of supercritical toppling energies, we predict $\alpha_X < 0.20$. This was not apparent from Fig. 1 where the peaks in the distribution of energy differences between neighboring sites appeared to lie approximately at multiples of $\alpha=0.20$. We note that, while this is a necessary condition, it is not sufficient to ensure all sites topple at the threshold in the infinite-size limit. This demonstrates that examination of the distribution of energy differences alone is a poor technique for identifying α_X . Similarly,

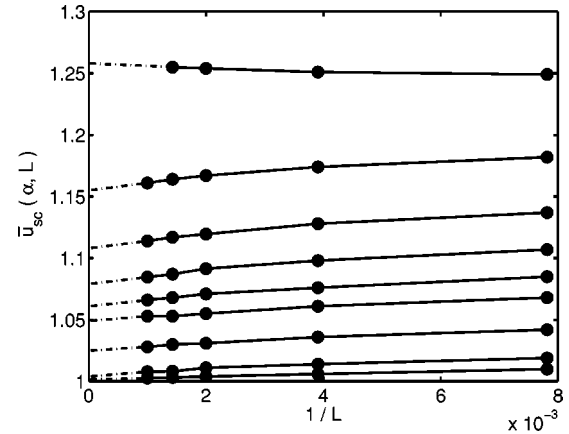


FIG. 3. The average supercritical toppling energy $\bar{u}_{sc}(\alpha, L)$ for various system sizes $128 \leq L \leq 1000$, and a range of conservation levels. From top to bottom the cases shown are $\alpha=0.25, 0.24, 0.23, 0.22, 0.21, 0.20, 0.18, 0.15$, and 0.13 . Error bars lie within the symbols. The dot-dash lines denote the extrapolation to infinite-system size.

for decreasing α it is increasingly difficult to accurately deduce the $L \rightarrow \infty$ distribution of supercritical toppling energies, P_{sc} , from finite-size simulation studies. When $\alpha=0.18$ there is clear evidence that the limiting distribution remains nonzero over a finite range of u_{sc} values, while for $\alpha=0.11$ we only observe a δ peak at $u_{sc}=1$ in the $L \rightarrow \infty$ limit. For intermediate values, we cannot make a conclusive identification of the limiting behavior from the finite-size system data available, and hence at this stage we identify $0.11 < \alpha_X < 0.18$. In order to more accurately determine the crossover value, we consider some alternative approaches below and in Sec. III.

Extrapolation to the infinite-size limit is more easily achieved by focusing on the average toppling value, rather than trying to extrapolate the entire supercritical distribution discussed above. In particular, we calculate the average toppling energy $\bar{u}_{sc}(\alpha, L)$ for a range of conservation levels α , and system-sizes L . In Fig. 3, we plot $\bar{u}_{sc}(\alpha, L)$ against $1/L$ and extrapolate to the infinite-size limit, for various α . For fixed α , as the system-size increases $\bar{u}_{sc}(\alpha, L)$ decreases, except in the conservative case. For the larger system-sizes considered our data lie on approximately straight lines suggesting extrapolation is a valid approach, and leading to the results shown in Fig. 4 for $\bar{u}_{sc}(\alpha, L \rightarrow \infty)$. For $\alpha \geq 0.16$ the limiting value of \bar{u}_{sc} is strictly greater than 1, and for $\alpha \leq 0.12$ the limiting value is identically 1 within the level of precision of the simulations. For $\alpha=0.15$ an extrapolated value of $\bar{u}_{sc}(\alpha, L \rightarrow \infty) = 1$ lies within our error bars, and so larger systems would need to be simulated in order to positively determine if $\alpha_X < 0.15$. However, on the basis of this study we predict $\alpha_X = 0.14 \pm 0.02$. We comment that the results given in this section are identical when either double- or quadruple-precision arithmetic is used for the simulations, suggesting that these findings will not be affected by further increasing precision.

Finally, in this section, we note that there is a qualitative

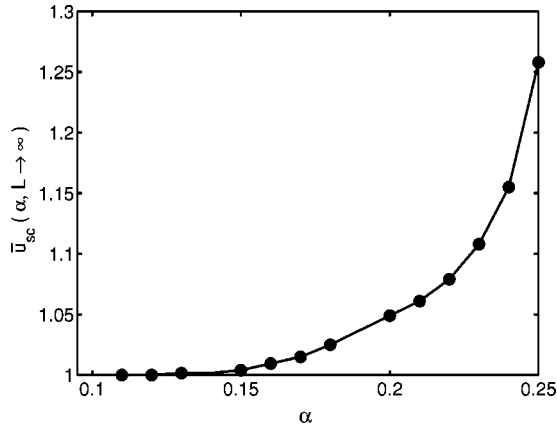


FIG. 4. Infinite-system-size limit of \bar{u}_{sc} plotted as a function of α . The error bars, corresponding to the range of extrapolated values consistent with the available finite-size system data, all lie within the symbols.

difference in the behavior of $\bar{u}_{sc}(\alpha, L)$ between the conservative case $\alpha=0.25$ and dissipative choices where $\alpha < 0.25$. This is clearly observed in Fig. 3, where one finds that the gradients of the lines in the two regimes have different signs. This indicates there may be some universal features of dissipative systems in the OFC model, an issue we discuss further in Sec. IV.

III. BOUNDS ON THE CROSSOVER VALUE

To check our results, we consider some methods of bounding α_X , which also allow us to further test the effect of altering the floating-point precision used in the simulations. First, we have looked at the percentage of avalanches which are of size 1, $N_1(\alpha, L)$ say, for a range of α and L values, and for different levels of precision. Since the rounding errors associated with finite precision are predicted to lead to a sequence of avalanches of size 1 being mistaken for a larger avalanche, the results for $N_1(\alpha, L)$ found from simulations are anticipated to consistently underestimate their infinite-precision counterparts. Our results for simulations performed using double-precision arithmetic are shown in Fig. 5. Note that the data typically lie on straight lines so extrapolation to the infinite-size limit is again reasonable. The $L \rightarrow \infty$ results are plotted in Fig. 6, and can be extrapolated to yield a lower bound for the crossover value, $\alpha_X^< \approx 0.08$, i.e., using double-precision arithmetic, we would anticipate that the probability of avalanches greater than 1 decays to zero for $\alpha < \alpha_X^<$ and $L \rightarrow \infty$. We have repeated this process using quadruple-precision arithmetic in the simulations. The results for $N_1(\alpha, L \rightarrow \infty)$ are also shown in Fig. 6, leading to a larger estimate for the lower bound as expected with increasing precision. In particular, we estimate $\alpha_X^< \approx 0.12$ in the quadruple-precision case, which is our best available estimate for the lower bound.

Finally, we have looked to find a corresponding upper bound $\alpha_X^>$ for the crossover value. To do this, we have recorded the percentage of toppling sites, $N_{th}(\alpha, L)$, whose

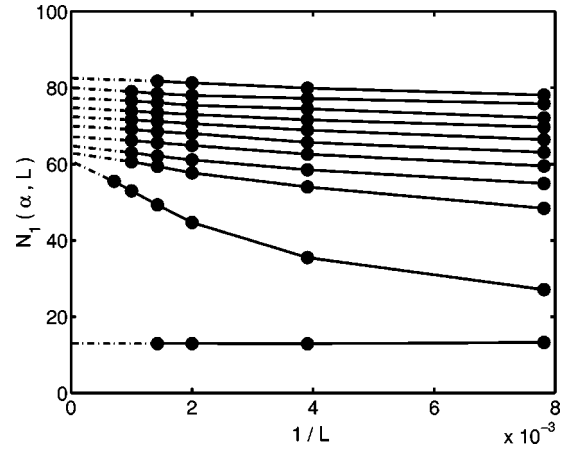


FIG. 5. The percentage of avalanches of size 1, $N_1(\alpha, L)$, plotted as a function of $1/L$. The data shown have been found from simulations using double-precision arithmetic. From top to bottom the cases shown are $\alpha=0.15, 0.16, \dots, 0.24, 0.25$. The dot-dash lines denote the extrapolation to infinite-system size.

toppling value lies in a range close to the threshold, $u_{sc} \in [1, 1 + \Delta]$ say. If the probability of avalanches greater than 1 vanishes in the infinite-size and infinite-precision limit then N_{th} will tend to 100%. In a finite-precision calculation some sites may topple in larger avalanches due to rounding errors as discussed above. However, such sites will have toppling values close to 1 and so will be included in N_{th} . In contrast some sites may genuinely topple with $u_{sc} \in (1, 1 + \Delta]$ in the infinite-precision, infinite-size limit and hence, we overestimate the percentage of sites actually toppling at the threshold value, leading to an upper bound $\alpha_X^>$. We have examined the results in both double and quadruple precision (with $\Delta = 10^{-12}$ and 10^{-28} , respectively). The results are qualita-

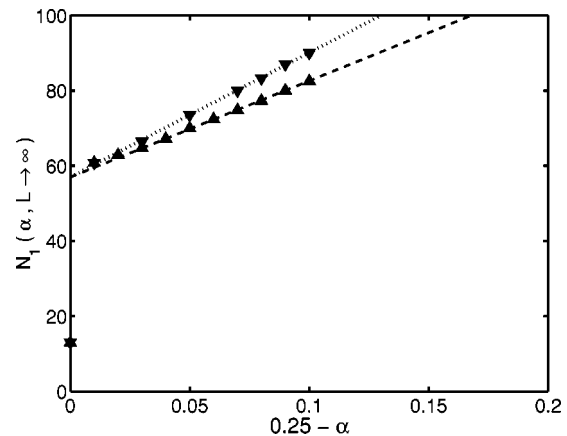


FIG. 6. Extrapolated infinite-size limiting results for N_1 plotted as a function of $0.25 - \alpha$. Results using double-precision (up-triangles) and quadruple-precision (down-triangles) arithmetic are shown, and are indistinguishable for the cases $\alpha=0.24$ and $\alpha=0.25$. The dotted and dashed lines are provided as a guide for the eye, while error bars (giving the range of extrapolated values consistent with available finite-size system data) lie within the symbols.

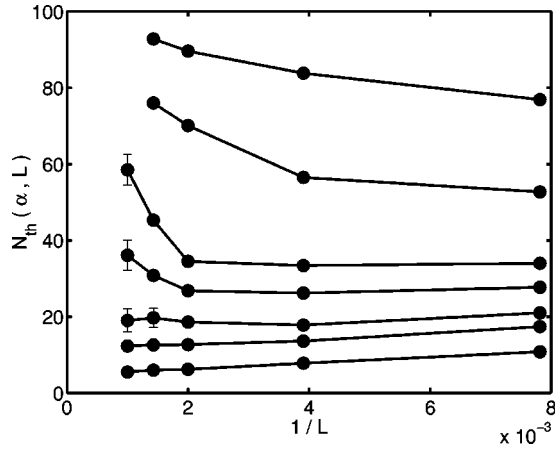


FIG. 7. The percentage of avalanches $N_{\text{th}}(\alpha, L)$ with toppling value $u_{sc} \in [1, 1 + 10^{-28}]$ plotted as a function of $1/L$. Quadruple-precision arithmetic simulations have been used, and error bars lie within the symbols unless otherwise shown. From top to bottom the curves correspond to $\alpha = 0.11, 0.13, 0.15, 0.16, 0.17, 0.18,$ and 0.20 .

tively similar with the quadruple-precision values consistently lower than their double-precision counterparts as expected. In Fig. 7, we plot $N_{\text{th}}(\alpha, L)$ for a range of α and L for the quadruple-precision case. For small α , e.g., $\alpha = 0.11$, the data extrapolates to 100% in the infinite-size limit, while for $\alpha \geq 0.17$ we find that N_{th} clearly does not approach 100%. For $0.13 < \alpha < 0.16$ a linear extrapolation over the larger system-sizes tends towards a limit below 100%, however, given the curvature of the lines one cannot reliably extrapolate in this range. Using double-precision arithmetic one finds the curvature is generally more pronounced for large L in comparison with Fig. 7. Furthermore, in double precision there is also curvature in the $\alpha = 0.17$ data resulting in a larger prediction for $\alpha_X^>$ than found from quadruple-precision simulations. Hence, we anticipate that if we could further increase precision our estimate for the crossover upper bound would decrease. However, on the basis of our available data our best estimate for the upper bound is $\alpha_X^> \approx 0.16$. Thus, we have shown in this section that on the basis of linear extrapolation the true value for α_X lies in the range $0.12 \leq \alpha_X \leq 0.16$, fully consistent with the findings based on the average supercritical toppling value described in Sec. II. Naturally, one must be wary of using extrapolation methods to determine $L \rightarrow \infty$ behavior since it may miss slow changes in slope, we consider alternative interpretations of the data in Sec. IV.

IV. SUMMARY AND CONCLUSIONS

We have used a variety of methods to numerically investigate the proposal that for the OFC model there exists a nonzero crossover value α_X below which the probability of observing avalanches of size greater than 1 vanishes in the asymptotic limit of both infinite system-size and infinite-precision arithmetic. We have identified that such a crossover

exists, and from a study of the average supercritical toppling energy predict $\alpha_X \approx 0.14$. Further, we have determined upper and lower bounds for the crossover value allowing us to explicitly analyze the effect of changing the level of floating-point precision in our simulations. We find $0.12 \leq \alpha_X \leq 0.16$, consistent with the earlier analysis of Drossel which predicts $0.10 \leq \alpha_X < 0.25$ [9].

In the limit of an infinite-size system and infinite-precision arithmetic, the probability of an avalanche of size greater than one is identically zero for $\alpha < \alpha_X$. In this region, a neighbor of the toppling site is frequently found to have its energy raised arbitrarily close to the threshold, and hence itself topples arbitrarily soon after the driving phase recommences. Thus, an analytic solution of the OFC model would find no event size distribution for $\alpha < \alpha_X$. However, in an experimental study (e.g., measuring earthquake or landslide event size distributions) there will be an observation time scale over which measurements are taken. A series of small events which occur over a very short time period will be measured as simultaneous, thus the observation time scale may yield a similar mechanism to finite-precision arithmetic in the simulations (i.e., allowing a sequence of single-size avalanches arbitrarily close to one another to be mistaken for one or more large avalanches). Thus, we believe the presence of a nonzero α_X value in the OFC model should not be viewed as a failing of the model in attempting to explain the abundance of power-law distributions observed in nature.

Finally, we note that many of our results show a qualitatively different behavior for the conservative regime compared to the dissipative cases. Most notably, the $L \rightarrow \infty$ limiting values for $N_1(\alpha, L)$ can all be fit, for a given choice of precision, by a simple linear function with the exception of the conservative system $\alpha = 0.25$ (see Fig. 6). Similarly the slopes for $\bar{u}_{sc}(L)$ (Fig. 3) and $N_1(\alpha, L)$ (Fig. 5) take different signs in the conservative and nonconservative cases, with the differences becoming more significant as the system size L is increased. This may indicate that $\alpha = 0.25$ separates two distinct types of behavior in the OFC model. One possibility is that the critical value $\alpha_c = 0.25$, in which case these results would provide support for recent claims that criticality is special to the conservative limit, with all dissipative systems sharing some universal, noncritical features [10,11]. An alternate possibility is that the crossover value $\alpha_X = 0.25$. This is outside the range we have predicted on the basis of linear extrapolation techniques, but as noted earlier when using extrapolation one can never be sure that simulations of still larger systems would not lead to different conclusions. Hence, one should not rule out the possibility that the qualitative difference in conservative and dissipative behavior is an indicator of $\alpha_X = 0.25$. Note that if this is the case one would again predict $\alpha_c = 0.25$ since $\alpha_c \geq \alpha_X$.

ACKNOWLEDGMENT

This research was supported in part by The Royal Society, U.K.

- [1] P. Bak, C Tang, and K. Wiesenfeld, *Phys. Rev. Lett.* **59**, 381 (1987); *Phys. Rev. A* **38**, 364 (1988).
- [2] An excellent review of the field is provided in H.J. Jensen, *Self-Organized Criticality* (Cambridge University Press, Cambridge, 1998).
- [3] T. Hwa and M. Kardar, *Phys. Rev. Lett.* **62**, 1813 (1989); S.S. Manna, L.B. Kiss, and J. Kertész, *J. Stat. Phys.* **61**, 923 (1990).
- [4] Z. Olami, H.J.S. Feder, and K. Christensen, *Phys. Rev. Lett.* **68**, 1244 (1992); K. Christensen and Z. Olami, *Phys. Rev. A* **46**, 1829 (1992).
- [5] R. Burridge and L. Knopoff, *Bull. Seismol. Soc. Am.* **57**, 341 (1967).
- [6] J.E.S. Socolar, G. Grinstein, and C. Jayaprakash, *Phys. Rev. E* **47**, 2366 (1993).
- [7] P. Grassberger, *Phys. Rev. E* **49**, 2436 (1994).
- [8] A.A. Middleton and C. Tang, *Phys. Rev. Lett.* **74**, 742 (1995).
- [9] B. Drossel, *Phys. Rev. Lett.* **89**, 238701 (2002).
- [10] J.X. de Carvalho and C.P.C. Prado, *Phys. Rev. Lett.* **84**, 4006 (2000).
- [11] G. Miller and C.J. Boulter, *Phys. Rev. E* **66**, 016123 (2002).
- [12] K. Christensen, D. Hamon, H.J. Jensen, and S. Lise, *Phys. Rev. Lett.* **87**, 039801 (2001); J.X. de Carvalho and C.P.C. Prado, *ibid.* **87**, 039802 (2001).
- [13] S. Bottani and B. Delamotte, *Physica D* **103**, 430 (1997).